

MOL (#22731)

Title page

Mechanisms of cardiolipin oxidation by cytochrome c: relevance to pro- and anti-apoptotic functions of etoposide.

**Yulia Y. Tyurina, Vidisha Kini, Vladimir A. Tyurin, Irina I. Vlasova, Jianfei Jiang,
Alexander A. Kapralov, Natalia I. Belikova, Jack C. Yalowich, Igor V. Kurnikov,
Valerian E. Kagan**

Center for Free Radical and Antioxidant Health, Departments of Environmental and Occupational Health (Y.Y.T., V.K., V.A.T., I.I.V., J.J., A.A.K., N.I.B., J.C.Y., I.V.K., V.E.K.); and Pharmacology (J.C.Y., V.E.K.) University of Pittsburgh, Pittsburgh, PA 15219.

MOL (#22731)

Running title page

Running title: Etoposide inhibition of cardiolipin oxidation

Corresponding author: E. Kagan, Ph.D., D. Sci.

Center for Free Radical & Antioxidant Health, Department of EOH

Bridgeside Point, 100 Technology Drive, Suite 350, Pittsburgh, PA 15219

Telephone: 412-624-9479; Fax: 412-624-9361; Email:(vkagan@eoh.pitt.edu).

Text pages – 25

Tables – 0

Schema – 1

Figures – 6

References – 40

Abstract – 273 words

Introduction – 642 words

Discussion – 1,476 words

Abbreviations used: DTPA, diethylenetriaminepentaacetic acid; AMVN, 2,2'-Azo-bis(2,4-dimethylvaleronitrile); PE, phosphatidylethanolamine; PAPC, 1-Palmitoyl-2-Arachidonoyl-*sn*-Glycero-3-Phosphocholine; PAPS, 1-Palmitoyl-2-Arachidonoyl-*sn*-Glycero-3-[Phospho-L-Serine]; TLCL, 1,1',2,2'-tetralinoleoyl-cardiolipin; TOCL, 1,1',2,2'-tetraoleoyl-cardiolipin; CL-OOH, cardiolipin hydroperoxides; etoposide, demethylepipodophyllotoxin-ethylenediene-glucopyranoside), SDS, sodium dodecyl sulfate; EPR, electron paramagnetic resonance; ROS, reactive oxygen species; phosphate buffered saline, PBS; high performance thin layer chromatography, HPTLC; high performance liquid chromatography, HPLC.

MOL (#22731)

Abstract

Execution of apoptotic program in mitochondria is associated with accumulation of cardiolipin peroxidation products required for the release of pro-apoptotic factors into the cytosol. This suggests that lipid antioxidants capable of inhibiting cardiolipin peroxidation may act as anti-apoptotic agents. Etoposide, a widely-used anti-tumor drug and a topoisomerase II inhibitor, is a prototypical inducer of apoptosis and, at the same time, an effective lipid radical scavenger and lipid antioxidant. Here, we demonstrate that cardiolipin oxidation during apoptosis is realized not via a random cardiolipin peroxidation mechanism but rather proceeds as a result of peroxidase reaction in a tight cytochrome *c*/cardiolipin complex that restrains interactions of etoposide with radical intermediates generated in the course of the reaction. Using low temperature and ambient temperature electron paramagnetic resonance spectroscopy of H₂O₂ induced protein derived (tyrosyl) radicals and etoposide phenoxyl radicals, respectively, we established that cardiolipin peroxidation and etoposide oxidation by cytochrome *c*/cardiolipin complex takes place predominantly on protein derived radicals of cytochrome *c*. We further show that etoposide can inhibit cytochrome *c* catalyzed oxidation of cardiolipin competing with it as a peroxidase substrate. Peroxidase reaction of cytochrome *c*/cardiolipin complexes causes cross linking and oligomerization of cytochrome *c*. With non-oxidizable tetraoleoyl-cardiolipin the cross-linking occurs via dityrosine formation, while bifunctional lipid oxidation products generated from tetralinoleoyl-cardiolipin participate in the production of high-molecular weight protein aggregates. Protein aggregation is effectively inhibited by etoposide. The inhibition of cardiolipin peroxidation by etoposide, however, is realized at far higher concentrations than those at which it induces apoptotic cell death. Thus, oxidation of cardiolipin by cytochrome *c*/

MOL (#22731)

cardiolipin peroxidase complex, which is essential for apoptosis, is not inhibited by pro-apoptotic concentrations of the drug.

Introduction

Mitochondria play a central role in the execution of apoptotic program realized through intrinsic mechanisms and extrinsic pathways in type II cells (Scaffidi et al., 1998). It is well documented that one of the early mitochondrial responses to pro-apoptotic stimuli is the generation of reactive oxygen species (ROS) (Raha and Robinson, 2001). While the overall significance of ROS production in apoptosis has been established by its inhibition by different antioxidant enzymes and free radical scavengers (Genova et al., 2003; Nomura et al., 1999), specific ROS-dependent mechanisms of apoptosis are still elusive. We have recently demonstrated that cytochrome *c* acts as a redox catalyst in oxidizing a mitochondria-specific phospholipid, cardiolipin, thus facilitating accumulation of cardiolipin hydroperoxides (CL-OOH) required for the release of pro-apoptotic factors from mitochondria into the cytosol (Kagan et al., 2004; Kagan et al., 2005). This suggests that free radical scavengers, particularly lipid antioxidants, capable of inhibiting cardiolipin oxidation may affect apoptotic responses of cells.

Etoposide, a widely-used anti-tumor drug and a topoisomerase II inhibitor, induces apoptosis accompanied by mitochondrial ROS production (Gorman et al., 1997; Pham and Hedley, 2001). At the same time, we and others have reported that etoposide is an effective scavenger of lipid radicals propagating lipid peroxidation (Kagan et al., 2001; Kalyanaraman et al., 1989; Tyurina et al., 2004) and as such it should suppress apoptosis. Thus both pro- and anti- apoptotic properties may be realized during etoposide induced apoptosis.

MOL (#22731)

During apoptosis, cardiolipin oxidation can proceed predominantly through an enzymatically catalyzed mechanism whereby cytochrome *c*/cardiolipin complex acts as a cardiolipin-specific oxygenase inserting hydroperoxide groups in one or more of the four polyunsaturated fatty acid residues of cardiolipin (similar to cyclooxygenase-catalyzed oxygenation of arachidonic acid (Egan et al., 1976)). Alternatively, the cytochrome *c*/cardiolipin complex can be involved only in catalytic initiation of cardiolipin oxidation followed by a non-enzymatic propagation of free radical cardiolipin oxidation, similar to well known mechanisms of peroxidation of polyunsaturated lipids in biomembranes (Kagan, 1988). Moreover, different reactive intermediates of the peroxidase reaction (heme-centered compounds I and II as well as of amino acid radicals formed by oxidation of protein residues) can be involved in lipid oxidation. Given the important role of cardiolipin oxidation in apoptosis (Garcia Fernandez et al., 2002; Ott et al., 2002; Petrosillo et al., 2003; Zamzani and Kroemer, 2003), characterization of the molecular mechanism of this reaction is important for regulation of apoptosis and development of targeted anti-apoptotic therapeutic interventions.

Lipid antioxidant action of etoposide yields etoposide phenoxyl radicals that have very low reactivity towards lipids but relatively high reactivity towards ascorbate, GSH, and protein cysteines (Kagan et al., 2001). Thus, etoposide is an excellent and specific lipid antioxidant that does not protect other important biomolecules against oxidation (Kagan et al., 1994; Yalowich et al., 1996). Hence, probing lipid oxidation pathways of apoptosis with etoposide is specific and is not likely to interfere with the other redox-sensitive mechanisms of apoptosis (Tyurina et al., 2004). In the current work, we attempted to discriminate between the two mechanisms of cardiolipin oxidation by monitoring the generation of CL-OOH as well as cytochrome *c* derived radicals in model systems and correlating them with the development of etoposide triggered

MOL (#22731)

apoptosis in cells. We now demonstrate that cardiolipin oxidation during apoptosis is not likely realized via a random cardiolipin peroxidation mechanism but rather proceeds as a result of peroxidase reaction in a tight cytochrome *c*/cardiolipin complex that restrains interactions of etoposide with radical intermediates generated in the course of the reaction. We further show that etoposide can inhibit cytochrome *c* catalyzed oxidation of cardiolipin competing with it as a peroxidase substrate. These inhibitory effects of etoposide, however, are realized at far higher concentrations than those at which it induces apoptotic cell death. Thus, oxidation of cardiolipin by cytochrome *c*/cardiolipin peroxidase complex, which is essential for apoptosis, is not inhibited by pro-apoptotic concentrations of the drug.

Materials and Methods

Chemicals. Etoposide (demethylepipodophyllotoxin-ethylenediene-glucopyranoside), microperoxidase 11, cytochrome *c*, sodium dodecyl sulfate (SDS), butylated hydroxytoluene, diethylenetriaminepentaacetic acid (DTPA), ethylene glycol-bis(b-aminoethylether)-N,N,N',N'-tetraacetic acid tetrasodium (EGTA), catalase, porcine pancreas-derived phospholipase A₂, digitonin were purchased from Sigma Aldrich (St. Louis, MO). Amplex Red (N-acetyl-3,7-dihydroxyphenoxazine) reagent was obtained from Molecular Probes (Eugene, OR). HPLC grade solvents, fetal bovine serum, RPMI 1640 with phenol red, RPMI 1640 without phenol red, phosphate buffered saline (PBS) and cocktail protease inhibitor were purchased from Invitrogen (Carlsbad, CA). Caspase Glow[®] 3/7 detection kit was purchased from Promega (Madison, WI). PAPC, 1-Palmitoyl-2-Arachidonoyl-*sn*-Glycerol-3-Phosphocholine, PAPS, 1-Palmitoyl-2-Arachidonoyl-*sn*-Glycerol-3-[Phospho-L-Serine], TLCL, 1,1',2,2'-tetralinoleoyl-cardiolipin, TOCL, 1,1',2,2'-tetraoleoyl-cardiolipin were obtained from Avanti Polar Lipids,

MOL (#22731)

Inc. (Albaster, AL). Azo-initiator, 2,2'-azo-bis(2,4-dimethyl-valeronitrile) (AMVN) was from Wako Chemicals U.S.A (Richmond, VA). Gel Code SilverSNAP stain Kit II was purchased from Pierce (Rockford, IL), NO donor, (Z)-1-[N-3-aminopropyl)-N-(n-propyl) amino] diazen-1-ium-1,2-diolate (PAPANONOate) was from Cayman Chemical Co. (Ann Arbor, MI).

Cell culture. HL-60 human promyelocytic leukemia cells (American Type Culture Collection) were grown in RPMI 1640 with phenol red supplemented with 12.5% heat inactivated fetal bovine serum at 37°C in a humidified atmosphere (5% CO₂ plus 95% air). Cells from passages 45-50 were used for the experiments. The density of the cells at collection time was 0.5 X 10⁶ cell/ml. HL-60 cells were incubated with either AMVN (500 µM) or etoposide (25 µM) or both together in fetal bovine serum-free RPMI 1640 medium without phenol red for 2h at 37°C.

Caspase-3/7 activity was measured using a luminescence Caspase-Glo[®] 3/7 assay kit (Promega, Madison, WI). Briefly, 50 µl of cell homogenates (20 µg protein) were mixed with 50 µl of Caspase-Glo[®] reagent and incubated at room temperature for 1 h. At the end of incubation, luminescence of each sample was measured using a plate reading chemiluminometer ML1000 (Dynatech Laboratories). Activity of caspase-3/7 was expressed as luminescence arbitrary units (LAU) per mg protein.

Cytochrome c release. Cells were resuspended in lysis buffer containing 250 mM sucrose, 20 mM HEPES-KOH (pH 7.5), 10 mM KCl, 1.5 mM MgCl₂, 1mM EDTA, 1 mM EGTA, 1 mM DTT, 1 mM PMSF, 1 µg/mL aprotinin, 1 µg/mL leupeptin and 0.05% digitonin for 3 min on ice. Samples were then centrifuged at 8 000 g for 5 min at 4 °C. Supernatants were collected as

MOL (#22731)

the cytosol fraction. Aliquots of 40 μg of cytosol fraction were examined on 12% of SDS-PAGE with anti-cytochrome *c* antibody (1:2000) (BD Pharmingen, San Jose, CA).

Preparation of liposomes. Small unilamellar liposomes containing 50% PC and 50 % TOCL or TLCL were produced as previously described (Kagan et al., 2005; Tyurina et al., 2004). Individual phospholipids, stored in chloroform were dried under N_2 . PBS containing 100 μM DTPA was added to obtain the phospholipid concentration of 200 μM , and the lipid mixture was vortexed and sonicated for 3 min under nitrogen on ice. All liposomes were used immediately after preparation. For the measurements of EPR spectra of etoposide phenoxyl radical at room temperature liposomes were prepared in N_2 -buffer and stored under N_2 .

Oxidation of phospholipids in liposomes. Liposomes were incubated with etoposide (1, 3, 5, 10, 25, 50 and 100 μM) for 15min on ice. Samples were treated with 250 μM AMVN or with cytochrome *c* (4 μM) and H_2O_2 (100 μM) for 1h at 37°C in a water bath. H_2O_2 was added four times (every 15 min) during the incubation period. Catalase (2 U) was added to eliminate residual H_2O_2 . In some experiments, liposomes (1.5 mM DOPC/TLCL at a ratio of 1:1) were pre-incubated with etoposide (7.5-700 μM) and then were treated with cytochrome *c* (30 μM) and H_2O_2 (100 μM , H_2O_2 was added four times (every 15 min) during the incubation period) for 1h at 37°C in a water bath. Lipids were then extracted in chloroform:methanol (2:1, v/v) solvent. The extracted lipids were used to determine phosphorus content and measure the amount of lipid hydroperoxides generated as documented below.

MOL (#22731)

Two-dimensional high performance thin layer chromatography (2D-HPTLC). The extracted lipids (either from cells or liposomes) were dried under nitrogen and separated by 2D-HPTLC on silica G plates. The plates were first developed with a solvent system consisting of chloroform : methanol : 28% ammonium hydroxide (65:25:5, v/v). After drying the plates with a forced air blower to remove the solvent, the plates were developed in the second dimension with a solvent system consisting of chloroform : acetone : methanol : glacial acetic acid : water (50:20:10:10:5, v/v). The phospholipids were visualized by exposure to iodine vapors and identified by comparison with migration of authentic phospholipid standards. The spots identified by iodine staining were scraped, and the silica was transferred to tubes. Lipid phosphorus was determined by the sub-micro method as previously described (Tyurina et al., 2004). The identity of each phospholipid was established by comparison with the R_f values measured for authentic standards.

Assay for phospholipid peroxidation. Lipid extracts were dried under nitrogen and then incubated with 100 μ l buffer containing 25 mM NaH₂PO₄, 0.5 mM EGTA and 1 mM calcium (pH 8.0), 10 μ l of 5 mM SDS and 1 μ l phospholipase A₂ for 30 min at room temperature. Two μ l of 1mM HCl and 1 mM EGTA were added to adjust the pH of the samples. 1.5 μ l of Amplex red (50 μ M) and microperoxidase 11(1 μ g/ μ l) solution was added and incubated on ice for 40 min. Reaction was stopped using 100 μ l of stop reagent (solution of 10 mM HCl, 4 mM butylated hydroxytoluene in ethanol). The samples were centrifuged at 15,000x g for 5min and the supernatant was used for HPLC analysis. Aliquots (5 μ l) were injected into a C-18 reverse phase column (Eclipse XDB-C18, 5 μ m, 150 x 4.6 mm). The column was eluted by mobile phase composed of 25 mM NaH₂PO₄ (pH 7.0) : methanol (60:40 v/v.) with 1ml/min flow rate.

MOL (#22731)

Lipid phosphorus was determined by a micro-method. The resorufin (an Amplex Red oxidation product) fluorescence was measured at 590 nm after excitation at 560 nm using a Shimadzu LC-100AT *vp* HPLC system equipped with fluorescence detector (model RF-10Ax1) and autosampler (model SIL-10AD *vp*).

Mass spectrometry of TLCL oxidation products. Electrospray ionization mass spectrometry (ESI-MS) of lipids was performed by direct infusion into a triple quadrupole mass spectrometer TQ70 (Finnigan, San Jose, CA). Sheath flow was adjusted to 5 μ l/min and the solvent consisted of chloroform:methanol (1:2, v/v). The electrospray probe was operated at a voltage differential of -3.5 kV in the negative ion mode. Mass spectra for doubly charged cardiolipin species were obtained by scanning in the range of 400-950 M/z every 1.5 s and summing individual spectra. Source temperature was maintained at 70 °C.

EPR measurements. EPR spectra were recorded on JEOL-REIX spectrometer with 100 kHz modulation (Kyoto, Japan). Measurements at room temperature were performed under N₂ conditions in gas-permeable Teflon tubing (0.8 mm internal diameter, 0.013 mm thickness) obtained from Alpha Wire Corp. (Elizabeth, NJ). The tubing was filled with 60 μ l of sample, folded doubly and placed in an open 3.0 mm internal diameter EPR quartz tube. Etoposide phenoxyl radical spectra were recorded at 3350 G, center field; 50 G, sweep width; 10 mW, microwave power; 0.5 G, field modulation; 10³, receiver gain; 0.03 s, time constant; 4 min, scan time. The time course of etoposide radical EPR signals was obtained by repeated scanning of the part of the spectrum (3350 G, centered field; 5 G, sweep width; other instrumental conditions were the same).

MOL (#22731)

The time course of etoposide radical EPR signals was used to determine the rate of etoposide radical production. Recombination rate constant of etoposide radicals was estimated at $k_R = 1.2 \times 10^{-3} \text{ M}^{-1} \text{ s}^{-1}$ from the observation of the decay of EPR signal of etoposide radicals obtained by fast oxidation of etoposide in the presence of an excess of H_2O_2 and horseradish peroxidase. In the experiments described further concentration of etoposide radicals did not exceed $c_{\text{max}} = 1 \text{ } \mu\text{M}$. At these concentrations, the life-time of etoposide radical $t_{1/2} = 1/(k_R * c_{\text{max}}) \sim 340 \text{ s}$ was greater than the time of the experiment (240 s). Therefore, to compute the etoposide oxidation rate, we assumed that etoposide radicals were accumulated without recombination during the course of the experiment and the rate of etoposide radical production was proportional to the increase of EPR signal amplitude.

For low temperature EPR measurements of radicals (protein-derived or etoposide radicals), samples (150 μl) were placed into a Teflon tube (3.7 mm internal diameter) and immediately immersed in liquid nitrogen. Frozen samples were removed from the tube and stored in liquid nitrogen. EPR spectra of the frozen samples were detected at 77 K under the conditions: 3230 G, centered field; 100 G, sweep width; 5 G, field modulation; 1 mW, microwave power; 0.1 s, time constant; 4 min, time scan. Dependence of relative magnitude (% of the maximal magnitude) of EPR signals of radicals on square root from microwave power (mW) was presented as saturation curves. The spin-lattice relaxation time was determined by fitting the experimental curve of radical signal saturation to the theoretical one as previously described (Castner, 1959).

For low temperature EPR measurements of heme nitrosylated cytochrome c, ferro-cytochrome c (100 μM) was incubated with liposomes in the presence of NO-donor, PAPANONOate (500 μM), under N_2 at 37°C for 15 min. The reaction was stopped by freezing

MOL (#22731)

the samples in liquid nitrogen. Spectra were recorded at 77K under the following instrumental settings: 3200 G, center field, 500 G, scan range, 5 G, modulation amplitude; 10 mW, microwave power; 0.1 s, time constant; 4 min, scan time; 5×10^2 , receiver gain.

Fluorescence measurements of dityrosine formation. After incubating of 10 μ M cytochrome *c* with 250 μ M TOCL or TLCL liposomes in the presence of 100 μ M H₂O₂ in presence or absence of etoposide for 1h at 37°C, dityrosine fluorescence in digested samples was determined as described (Giulivi et al., 2003).

PAGE electrophoresis of cytochrome *c*/CL complexes. DOPC/CL liposomes (200 μ M, at a ratio of 1:1) were incubated with cytochrome *c* (4 μ M) in the presence of 100 μ M H₂O₂. Electrophoresis was performed in 12.5% PAGE. Gels were stained by silver using GelCode SilverSNAP Stain Kit II (Pierce). For Coomassie blue staining of the gels, the amounts of liposomes and cytochrome *c* were increased up to 1.5 mM and 30 μ M, respectively. To quantitatively evaluate cytochrome *c* aggregation, densitometry of stained protein bands on gels using Fluor-S Multimager (Bio-Rad, Hercules, CA) was performed. Protein bands from Coomassie Blue stained gels were excised and cut into smaller pieces. Destaining, digestion with trypsin and extraction of peptides was performed as described in (Jimenez et al., 1998). Dityrosine fluorescence was measured as described above.

Statistics. The results are presented as mean \pm S.E. values from at least three experiments, and statistical analysis were performed by either paired or unpaired Student's *t* test of one-way ANOVA. The statistical significance of difference was set at $p < 0.05$.

MOL (#22731)

Results

Effect of etoposide on phospholipid oxidation in HL-60 cells. We assessed lipid peroxidation in HL-60 cells treated with (for 2h at 37 °C): 1) a lipophilic azo-initiator of peroxy radicals, AMVN (2,2'-Azo-bis(2,4-dimethylvaleronitrile)) (500 μ M), 2) etoposide (25 μ M), and 3) a combination of AMVN plus etoposide. Phospholipids were extracted and separated by 2-dimensional HPTLC. A typical HPTLC separation profile is shown on Fig.1A. Phosphatidylcholine represented about one half of the total phospholipids with phosphatidylethanolamine (PE) being the next most abundant phospholipid class (about 20%). Additionally, the phospholipids in the order of their abundance - phosphatidylinositol > sphingomyelin > phosphatidylserine > cardiolipin - were detectable on the HPTLC plates. There were no significant differences in the pattern of distribution of phospholipid classes between treated and untreated HL-60 cells (data not shown). Spots corresponding to different phospholipids were scraped and the amounts of phospholipid hydroperoxides generated in HL-60 cells were determined using our newly developed fluorescence HPLC/Amplex Red-based assay (Kagan et al., 2005). We found that AMVN induced oxidation of all major classes of phospholipids, including phosphatidylcholine, PE, phosphatidylserine and cardiolipin (Fig. 1B). Etoposide alone caused a strong oxidation of cardiolipin while it did not induce oxidation of other more abundant phospholipid classes, in line with our previously published results (Tyurina et al., 2004). Moreover, when applied in a combination with AMVN, etoposide suppressed the AMVN-induced oxidation of all phospholipids - phosphatidylcholine, PE and phosphatidylserine – with a notable exception of cardiolipin. In fact, the AMVN-induced oxidation of cardiolipin was markedly enhanced by etoposide. These results indicate that there are profound differences in mechanisms of phospholipid oxidation by etoposide and AMVN in

MOL (#22731)

HL-60 cells that are likely associated with the apoptosis-specific pathways. Therefore, we next compared effects of AMVN, etoposide, and a combination of AMVN plus etoposide on oxidation of phospholipids in liposomes prepared from readily oxidizable polyunsaturated phospholipids, palmitoyl-arachidonoyl-phosphatidylcholine (PAPC), palmitoyl-arachidonoyl-phosphatidylserine (PAPS) and TLCL. Similarly to cells, AMVN induced oxidation of all phospholipids in liposomes (Fig. 1C). Expectedly, etoposide did not cause any oxidation of liposomal phospholipids. In contrast to HL-60 cells, however, etoposide equally protected all phospholipids, including cardiolipin, against AMVN-induced oxidation in liposomes, (Fig.1C). Because in these experiments, relatively low etoposide concentrations (25 μ M) were used that were sufficient to induce apoptosis in HL-60 cells (Fig.1D), these results clearly demonstrate that apoptosis-associated peroxidation of cardiolipin is not effectively quenched by etoposide. Notably, the conditions of AMVN exposure of HL-60 cells were well-suited for the induction of apoptosis. Therefore, both random oxidation of phospholipids by a radical initiator as well as apoptosis-specific oxidation of cardiolipin were triggered by AMVN. The ability of etoposide to induce cardiolipin oxidation in HL-60 cells both in the presence and in the absence of AMVN is related to its proapoptotic properties. Execution of apoptotic program is accompanied by the generation of ROS and lipid oxidation (Kagan et al., 2004; Raha and Robinson, 2001), that is catalyzed by cytochrome *c* molecules bound to cardiolipin-containing mitochondrial membranes (Kagan et al., 2005). Thus involvement of specific cytochrome *c*-dependent mechanisms in cardiolipin oxidation during apoptosis may be responsible, at least in part, for a decreased sensitivity of cardiolipin oxidation to inhibitory effects of radical scavengers like etoposide. Therefore, we further tested cardiolipin oxidation in the presence and absence of

MOL (#22731)

etoposide in a cell-free system, containing model cardiolipin membranes and cytochrome *c* molecules.

Effect of etoposide on cardiolipin oxidation in a model system. We compared the effectiveness of etoposide in inhibiting cardiolipin oxidation induced by a free radical generator AMVN with its ability to suppress cytochrome *c* catalyzed cardiolipin oxidation. To this end, we used liposomes containing dioleoylphosphatidylcholine (DOPC) and TLCL at a ratio of 1:1. TLCL was a natural choice since it is the most abundant cardiolipin species found in mammalian mitochondria (Schlame and Rustow, 1990). Liposomes were incubated in PBS (containing 100 μ M DTPA to prevent non-specific metal-catalyzed oxidation) for 1h at 37 °C with 250 μ M AMVN, which generates peroxy radicals at constant rate at a given temperature (Niki, 1990). At the end of the incubation, phospholipids were extracted, resolved by 1-dimensional HPTLC to separate etoposide from the phospholipids and the content of CL-OOH was determined using the Amplex Red fluorescence HPLC-based assay (Kagan et al., 2005). We found that incubation of liposomes with AMVN resulted in accumulation of up to 155.8 ± 13.0 pmol CL-OOH/nmol cardiolipin (~ 1.55 nmol/ml). This corresponds well with the total amount of radicals generated by AMVN (1.22 nmol/ml) during this period of time (3600 s) given that its decomposition rate is $1.36 \times 10^{-6} [\text{AMVN}] \text{ Ms}^{-1}$ (Niki, 1990). Addition of etoposide to the incubation system resulted in a significant decrease of cardiolipin oxidation the magnitude of which was proportional to etoposide concentration. Half-maximal inhibition (I_{50}) was achieved at ~ 3 μ M etoposide, whereas nearly complete inhibition was obtained at 25 μ M etoposide (Fig.2A). These results demonstrate that etoposide is an effective radical scavenger as has been demonstrated previously by us in other systems (Kagan et al., 2001).

MOL (#22731)

We next evaluated the potency of etoposide as an inhibitor of enzymatic cytochrome *c*/cardiolipin catalyzed oxidation. We chose the conditions (incubation of TLCL liposomes in PBS for 1h at 37 °C with cytochrome *c* (4 μM) and H₂O₂ (100 μM, added every 15min) yielding approximately the same cardiolipin oxidation level (162±38 pmol CL-OOH/nmol cardiolipin) as the one generated by the AMVN system (compare Fig.2A and 2B). While etoposide protected TLCL against enzymatic cytochrome *c* oxidation, its potency was approximately 5-fold lower with I₅₀ = 15 μM (Fig.2B). The lower antioxidant activity of etoposide in the cytochrome *c*/H₂O₂ system compared to AMVN induced cardiolipin oxidation is not entirely unexpected and may be related to its hindered interactions with reactive intermediates of cytochrome *c*/cardiolipin peroxidase complex (compound I, compound II, protein-derived (tyrosyl) amino acid radicals) as compared to stochastic interaction with lipid peroxy radicals during AMVN induced TLCL oxidation. To gain a better understanding of etoposide participation in cytochrome *c*/cardiolipin peroxidase reaction, we applied EPR spectroscopy to detect radical intermediates generated by the cytochrome *c*/cardiolipin complexes such as etoposide phenoxyl radicals as well as protein-derived (tyrosyl) radicals (Kalyanaraman et al., 1989).

EPR measurements of etoposide phenoxyl radical formation. Both non-enzymatic and enzymatic (e.g., peroxidases-catalyzed) one-electron oxidation of etoposide yields its phenoxyl radicals with characteristic signals in the EPR spectra (Kagan et al., 1999). Accordingly, incubation of TLCL liposomes with cytochrome *c*, etoposide and H₂O₂ (under N₂) produced a characteristic EPR signal of etoposide phenoxyl radical (Fig. 3Aa). This signal was not observed in the absence of H₂O₂ (data not shown). The magnitude of the signal increased over

MOL (#22731)

time and its growth was approximately linear over initial 4-5 min of incubation (Fig.3Ab). Assuming that changes in the magnitude of the signal are proportional to the etoposide radical production rate (see Materials and Methods for details) we assessed the rate of etoposide radical production at different concentrations of the drug in the presence of TLCL. Peroxidase activity of cytochrome *c*/TLCL can utilize both etoposide and TLCL as substrates resulting in TLCL hydroperoxide and etoposide radical formation, respectively. As shown on Fig. 3B, etoposide radical production increased and then saturated at etoposide concentrations higher than 100 μ M. This may be due to etoposide's ability to outcompete TLCL as a peroxidase substrate. We performed the same series of experiments with mono-unsaturated TOCL that does not undergo cytochrome *c*/H₂O₂ catalyzed peroxidation (see Fig. 3B, insert). In this case, saturation of the etoposide radical production was achieved at significantly lower etoposide concentrations (~50 μ M). The half maximum rate of etoposide oxidation was reached at concentrations of about 5 μ M in the presence of TOCL as compared to ~15 μ M for TLCL (Fig. 3B). These results indicate that cytochrome *c* is an effective catalyst of TLCL oxidation resulting in the requirement of high etoposide concentrations to block TLCL oxidation in line with the results of Fig. 2.

To further characterize the involvement of protein radicals in lipid peroxidation induced by cytochrome *c*/TLCL complex we performed low temperature EPR studies of cytochrome *c*/cardiolipin complexes in the presence of H₂O₂ and etoposide.

EPR measurements of protein-derived (tyrosyl) radical formation. Catalytic activation of peroxidases is known to form highly reactive oxidizing intermediates – compounds I and II (Lassmann et al., 1991). The production of the latter intermediate is also associated with the

MOL (#22731)

generation of another oxidizing species, an amino acid centered (often tyrosyl) radical detectable by EPR (Svistunenko, 2005; Tsai et al., 1999). Thermodynamically, any of these reactive intermediates of cytochrome *c*/cardiolipin peroxidase complex can oxidize etoposide to generate its phenoxyl radical (Buettner, 1993; Koppenol, 1990). EPR spectra of protein-derived (tyrosyl) radicals of cytochrome *c* at 77 K induced by high concentrations of oxidants have been reported (Chen et al., 2004a; Chen et al., 2004b; Lassmann et al., 1991). As shown in Fig.4A, a characteristic low temperature EPR signal of (tyrosyl) radical with peak-trough width of 16 G and $g = 2.005$ was readily detectable in cytochrome *c* /TOCL and cytochrome *c*/TLCL systems immediately upon addition of H_2O_2 . This signal was only barely detectable from cytochrome *c* plus H_2O_2 in the absence of TOCL or TLCL or from the mixture of cytochrome *c* with PC liposomes plus H_2O_2 (data not shown). The magnitude of the (tyrosyl) radical signal from cytochrome *c*/cardiolipin complex (Fig.4Ab) was about 30 ± 7 % lower for readily peroxidizable TLCL than for non-oxidizable TOCL (Fig.4A). It is likely that the difference is due to partial quenching of the (tyrosyl) radical by the involvement of the radical in oxidation of TLCL.

Addition of etoposide to either TOCL- or TLCL- complexes of cytochrome *c* (Fig.4Ac) resulted (in the presence of H_2O_2) in approximately two-fold increase of the magnitude of the EPR signal and change of its shape ($g = 2.005$ with a peak and trough width of 11.5 G). This seemingly “unexpected” growth of the signal may be explained by superposition of the protein-derived (tyrosyl) radical signal and the etoposide phenoxyl radical signal. In fact, as both of them have similar g -factors (2.005 and 2.005, respectively), and half-widths (16 G and 11.5 G, respectively), their simultaneous formation is likely to cause an increase of the overall EPR signal.

MOL (#22731)

To verify that reduced magnitude of the EPR signal detectable in the presence of TLCL did not relate to diminished generation of tyrosyl radicals we measured cytochrome *c* nitrosylation in the presence of TLCL and TOCL using low-temperature EPR spectroscopy. We found that incubation of cytochrome *c* with TOCL or TLCL in the presence of an NO donor, PAPANONOate, results in appearance of EPR spectra characteristic for heme-nitrosylated cytochrome *c* (Fig. 4B). Under the experimental conditions used, the magnitude and the shape of the EPR spectra were essentially the same. No significant spectra were observed in the absence of cardiolipins. Thus, interaction of cytochrome *c* with cardiolipins caused similar unfolding of the protein and similar accessibility of the cytochrome *c* heme to NO.

If oxidation of etoposide to its phenoxyl radical occurred on the protein-derived (tyrosyl) radical of cytochrome *c*/cardiolipin complex, one would expect to detect a decrease of its magnitude (due to its reduction by etoposide). Given very similar parameters for both of the signals - the protein-derived (tyrosyl) radical and etoposide phenoxyl radical – the reduction of tyrosyl radical by etoposide likely does not change the overall EPR signal magnitude. The observed large increase of the signal is in line with a longer life-span of etoposide phenoxyl radicals (100-1000 sec under our experimental conditions) compared to tyrosyl radicals (Chen et al., 2004a; Tsai et al., 1999). Consequently, steady-state concentrations of phenoxyl radicals are higher resulting in a greater magnitude of the EPR signal. This is also supported by our results on power saturation of etoposide phenoxyl radical and protein-derived (tyrosyl) radical EPR signals (Fig.4C). The etoposide phenoxyl radical EPR signal saturated at a significantly lower power of magnetic field than protein-derived (tyrosyl) radical signal. Power saturation of radical EPR signal depends very strongly on the distance between a radical and metal ion (Lassmann et

MOL (#22731)

al., 1991). To quantitate tyrosyl and phenoxyl radical saturation parameters, we evaluated the spin-lattice relaxation time that is sensitive to the radical interaction with paramagnetic metals, in two different systems: cytochrome *c*/TOCL + H₂O₂ and cytochrome *c*/TOCL + etoposide + H₂O₂. We found that the spin-lattice relaxation time for the tyrosyl radicals and phenoxyl radicals were substantially different and estimated as $T_1=(1.2\pm0.3)\times10^{-5}$ s and $T_1=(4.3\pm0.5)\times10^{-5}$ s, respectively.

Formation of dityrosines in cytochrome c peroxidase reaction. A protein-derived tyrosyl radical formed during peroxidase reaction of cytochrome *c*/cardiolipin complex is relatively long-lived and can isomerize and combine with another tyrosyl radical with subsequent enolization (Giulivi et al., 2003). As a result a stable, covalent, carbon–carbon bond is generated yielding 1,3-dityrosine. The latter is distinguished by the intense 420 nm fluorescence emission, measurable upon excitation at 315 nm (Malencik et al., 1996). Several oxidizing systems were found to produce dityrosines during oxidant exposure of both purified proteins *in vitro* and intact cells. We found a markedly increased fluorescence characteristic of dityrosines from cytochrome *c*/TOCL complex incubated in the presence of H₂O₂. The fluorescence response was quenched by etoposide in a concentration-dependent manner (Fig. 5A). Assuming that no dityrosines are formed at high etoposide concentrations (250 μM) and the fluorescence level at these conditions can be taken as a background, the half-maximal inhibition of dityrosine fluorescence quenching was achieved by the etoposide concentration of ~5 μM. This is consistent with the concentration dependence of etoposide radical formation shown on Fig. 3B. Notably, no characteristic dityrosine fluorescence was observed from cytochrome *c*/TLCL complexes treated with H₂O₂ in presence or absence of etoposide. This suggests that protein-

MOL (#22731)

derived tyrosyl radicals do not form dimers in the presence of readily oxidizable TLCL but rather participate in lipid peroxidation.

Detection of CL/cytochrome *c* oligomerization products by PAGE electrophoresis. Formation of dityrosine cross-links between cytochrome *c* molecules should be associated with the accumulation of different protein oligomers detectable on PAGE gels under denaturing conditions (Chen et al., 2004b). Indeed, when cytochrome *c*/TOCL complexes were incubated with H₂O₂, dimers, trimers, tetramers of cytochrome *c* and larger aggregates, which did not enter the gel due to their very high molecular weight, were observed - along with the monomeric species (Fig. 5B). Etoposide effectively inhibited oligomerization of cytochrome *c*/TOCL complexes, particularly the formation of very high molecular weight aggregates, thus preserving monomeric form of cytochrome *c* (Fig. 5C and D).

When ~8-times higher concentration of cytochrome *c* (30 μM) was used, a much higher concentration of etoposide (~350 μM, see Fig. 5B insert) was needed to prevent dityrosine formation in experiments with TOCL. We additionally studied the effects of etoposide on TLCL peroxidation in the same concentration range as for the assessments of dityrosine formation. We incubated TLCL/DOPC liposomes (1.5 mM) in the presence of cytochrome *c* (30 μM; note that the cytochrome *c* concentration in these was also higher) and H₂O₂ (100 μM added four times every 30 min during the incubation) and measured TLCL oxidation by Amplex Red procedure. Using different concentrations of etoposide (7.5-750 μM), we found that under these conditions I₅₀ for etoposide inhibition of cardiolipin peroxidation was ~150 μM (Fig.6A). Further, we verified the protective effect of high concentrations of etoposide (750 μM) against TLCL peroxidation using ESI-MS. Significant accumulation of monohydroperoxy/monohydroxy

MOL (#22731)

derivatives of TLCL as observed after the incubation in the absence of etoposide (M/z 724.2 + 8 = 732.2; 724.2 + 16 = 739.7; 724.2 + 24 = 748.2; 724.2 + 32 = 755.9; 724.2 + 40 = 763.8; 724.2 + 48 = 771.8; 724.2 + 56 = 779.7; 724.2 + 64 = 787.9; and 724 + 72 = 795.7). This effect was markedly reduced by etoposide (Fig.6B). These observations indicate that protein tyrosyl radicals are formed even at high (>100 μ M) concentration of etoposide, that are sufficient to prevent lipid peroxidation and etoposide exerts its antioxidant activity by interacting with tyrosyl radicals rather than with heme-centered compound I and II reactive intermediates.

The cytochrome *c*/TLCL complexes did not display the formation of di-, tri-, or tetra-oligomers of cytochrome *c* upon exposure to H_2O_2 . Instead only very high molecular weight aggregates that did not enter the gel accumulated (Fig. 5A). The dityrosine fluorescence of cytochrome *c* oligomeric cross-links formed in the presence of TOCL and TLCL after separation by PAGE. We found that cytochrome *c*/TOCL aggregates displayed higher levels of characteristic dityrosine fluorescence than aggregates formed during the incubation of cytochrome *c*/TLCL complexes with H_2O_2 (Fig. 5A, inset). These results suggest that oxidative oligomerization of cytochrome *c* in the presence of TLCL likely involves not only dityrosine cross-linking, typical of oligomerization in the presence of TOCL, but also additional mechanisms, possibly including cross-linking by bi-functional secondary products of lipid peroxidation (eg, di-aldehydes) (Kagan, 1988). A weaker silver-staining of very high molecular weight aggregates was observed in samples treated with etoposide. Quantitatively, this was confirmed by densitometry of protein bands performed using Fluor-S Multimager (Bio-Rad, Hercules, CA). Additional bands with molecular weights in the range of 30-40 kDa appeared in the presence of etoposide. Because the formation of dityrosine cross-links is realized through carbon-carbon bonds, the tyrosine hydroxy-functionalities remain available for multiple cross-

MOL (#22731)

linking. As a result, very high molecular weight aggregates may be produced. Our results suggest that etoposide was able to inhibit this multiple cross linking and the production of high molecular weight aggregates. However, lower molecular weight oligomers were still formed in detectable amounts in the presence of etoposide as documented by the gels.

Etoposide was able to significantly prevent accumulation of these high molecular weight cross-links (Fig. 5C inset). Thus, two different types of oligomerization products were formed from complexes of cytochrome *c* with either non-peroxidizable TOCL or readily peroxidizable TLCL. The former resulted from the production of dityrosine cross-links and exerted characteristic fluorescence while the latter were cross-linked by secondary lipid peroxidation products that did not exert characteristic di-tyrosine fluorescence. Etoposide was able to substantially inhibit aggregation of cytochrome *c* complexes with both TOCL and TLCL, although substantial formation of lipid-protein aggregates in TLCL experiments was still observed at etoposide concentration as high as 100 μ M, indicating that lipid and protein radicals formed as a result of peroxidase reaction in the tight cytochrome *c*/cardiolipin complex are protected against antioxidant activity of etoposide molecules.

Discussion

Generation of ROS and lipid peroxidation are two essential events in the execution of apoptotic program as evidenced by the ability of free radical scavengers and overexpressed antioxidant enzymes to suppress apoptosis (Genova et al., 2003; Nomura et al., 1999). Their specific mechanisms of action in apoptosis are still not completely understood. We have recently described a new catalytic role of cytochrome *c* as a specific cardiolipin-oxygenase acting at early mitochondrial stages of apoptosis to generate CL-OOH required for the release of

MOL (#22731)

pro-apoptotic factors into the cytosol (Kagan et al., 2005). This implies that lipid antioxidants capable of suppressing cardiolipin oxidation should be also effective as anti-apoptotic agents. Indeed, several studies have demonstrated anti-apoptotic properties of major lipid-soluble antioxidants such as vitamin E (Buettner, 1993) and ubiquinol (Kelso et al., 2001). We and others have reported high efficiency of etoposide as a specific lipid antioxidant (Tyurina et al., 2004) which, in contrast to the above prediction, is also known as a potent inducer of apoptosis. Therefore, we were anxious to discern why etoposide readily induces apoptosis notwithstanding its known antioxidant properties. In particular, we analyzed how the apparent inability of etoposide to prevent apoptosis but conversely to trigger it may be related to the mechanism of mitochondrial cardiolipin oxidation catalyzed by cytochrome *c*. Surprisingly, we found that cardiolipin was oxidized preferentially by etoposide at concentrations at which it induced apoptosis. In fact, the level of cardiolipin oxidation was higher than that induced by a pro-oxidant inducer of apoptosis, AMVN (that does not elicit antioxidant properties). Oxidation of other more abundant phospholipids was markedly lower in the case of etoposide induced apoptosis in comparison to AMVN induced apoptosis. Thus, etoposide was effective as a scavenger of phospholipid radicals but this scavenging activity could not be realized towards radical intermediates of cardiolipin oxidation. These findings indicated that oxidation of cardiolipin during apoptosis was executed through a different mechanism compared to oxidation of other phospholipids.

Our previous work has demonstrated that cardiolipin in mitochondria is oxidized mostly as a result of peroxidase reaction catalyzed by cytochrome *c* bound to cardiolipin-containing mitochondrial membranes (Kagan et al., 2005). In native cytochrome *c*, hexa-coordinate heme iron - with His₁₆ and Met₈₀ as axial ligands - cannot interact with small molecules, resulting in its

MOL (#22731)

very weak peroxidase activity and barely detectable EPR signal of tyrosyl radical in the presence of H_2O_2 . Both the activity and the signal may be associated with partial unfolding of the protein and a slow oxidation of Met₈₀ by H_2O_2 (Griffiths and Cooney, 2002). Notably, the magnitude of the H_2O_2 -induced EPR signal from solubilized cytochrome *c* is about 30-times lower than the signal from the cytochrome *c*/TOCL complex. Several lines of evidence suggest that cytochrome *c*, the heme protein that normally serves as an electron carrier and located in the intermembrane space of mitochondria, dramatically increases its peroxidase ability when it is bound to membranes containing negatively charged lipids, particularly cardiolipin. There are also indications that cardiolipin – which constitutes about 25% of phospholipids in the inner mitochondrial membranes - is normally located preferentially in the inner leaflet of the inner mitochondrial membrane (Robinson et al., 1990). However, during apoptosis cardiolipin is redistributed such that a significant fraction of it is found in the outer leaflet of the inner mitochondrial membrane as well as in the outer membrane (Garcia Fernandez et al., 2002; Robinson et al., 1990). Thus, physical interactions between cardiolipin and cytochrome *c* in apoptotic mitochondria are possible allowing for a switch in cytochrome *c*'s function from an electron carrier to a peroxidase with a high affinity for cardiolipin (Kagan et al., 2005). This explains the low efficiency of etoposide in inhibiting enzymatic (rather than random non-enzymatic) cardiolipin oxidation whereby cardiolipin radical intermediates are not readily accessible to radical scavengers, similarly to radicals formed during arachidonic acid oxidation by cyclooxygenases (Lassmann et al., 1991). Indeed, our *in vitro* studies showed very different protective effect of etoposide against random, free radical oxidation of cardiolipin and oxidation via peroxidation reaction catalyzed by cytochrome *c* bound to cardiolipin - containing liposomes. The decreased antioxidant potency of etoposide in the cytochrome *c*/cardiolipin/ H_2O_2 system can

MOL (#22731)

be attributed to a tight complex formed by cytochrome *c* and cardiolipin that insures close interactions of peroxidase reaction intermediates like compound I, compound II and amino-acid radicals with cardiolipin and prevent their inactivation by etoposide. These results also raise an important question about possible sites of etoposide interactions with radical intermediates generated by peroxidase activation of cytochrome *c*. Schema 1 presents possible pathways in the cytochrome *c*/cardiolipin catalyzed peroxidase reaction and interactions with etoposide.

The ability of etoposide to quench reactive species generated in the course of the peroxidase reaction, and to form etoposide radicals is maximal and similar for both TLCL and TOCL indicating that peroxidase reaction proceeded similarly for both cardiolipin species (the Schema 1).

Our results show that protein-derived radicals in the case of TLCL were quenched as compared to TOCL by 30 ± 7 %. This quenching may be the result of oxidation of TLCL by amino-acid radicals. A weak dityrosine formation was detected in TLCL experiments indicating that some of the protein radicals observed are inside the protein and cannot form dityrosine bridges, while protein surface tyrosine radicals are quenched by TLCL.

Recently, we demonstrated that peroxidase activity of cytochrome *c* complexes with TOCL and TLCL was the same as evidenced by two different assays based on H₂O₂ induced oxidation of 2',7'-dichlorodihydrofluorescein to 2',7'-dichlorofluorescein and of Amplex Red to resorufin (Kagan et al., 2005). Because peroxidase activity of cytochrome *c* is closely associated with the generation of tyrosyl radicals, we assumed that the production of the radicals is likely equivalent in the presence of either TOCL or TLCL. Moreover, according to our estimates, the binding constants of cytochrome *c* with TOCL and TLCL were essentially identical ($1.7 \pm 1.0 \times 10^9 \text{ M}^{-1}$ and $1.6 \pm 0.2 \times 10^9 \text{ M}^{-1}$, respectively (Belikova et al., 2006). Furthermore, our low-temperature

MOL (#22731)

EPR spectroscopy measurements revealed similar EPR signals of heme-nitrosylated cytochrome *c* complexes with TOCL or TLCL indicating the same accessibility of the cytochrome *c* heme to NO (Vlasova et al., 2006). Finally, the saturation behavior of tyrosyl radicals formed in the peroxidase reactions of cytochrome *c* complexes with TOCL and TLCL revealed the same distance from the heme iron. Combined, these results strongly suggest that a similar pattern of the protein-derived radical formation is characteristic of cytochrome *c* complexes with both cardiolipins. Thus, reduced magnitude of the EPR signal detectable in the presence of TLCL is unlikely due to diminished generation of tyrosyl radicals.

It has been reported previously (Chen et al., 2004a) that tyrosyl radicals formed as a result of tyrosine oxidation by peroxidase compounds I and II can be much more effective activators of lipid peroxidation than compounds I and II themselves. Cytochrome *c* has four tyrosine residues some of which are located close to the heme moiety and some are present on the surface of the protein. Interaction of cytochrome *c* with cardiolipin results in partial unfolding of the protein and tyrosine residues in the complex formed may readily interact with both heme and polyunsaturated lipid acyl chains. Thus formation of cytochrome *c*/cardiolipin complexes creates conditions for effective and specific cardiolipin peroxidation that is resistant to free radical scavengers such as etoposide.

The specificity of oxidation process can also be explained considering the redox potentials of redox species involved. Compound I and II with redox potentials of $\sim 0.95 - 1.0$ V (Buettner, 1993) are strong oxidants capable of oxidizing a wide range of substrates. Tyrosyl radical with $E^\circ = 0.7 - 0.9$ V (Buettner, 1993) can oxidize TLCL ($E^\circ = 0.6$ V) (Koppenol, 1990) and etoposide ($E^\circ = 0.56$ V) (Wardman, 1989). Monounsaturated TOCL has a higher redox potential ($E^\circ =$

MOL (#22731)

0.9V) (Wardman, 1989), and tyrosyl radicals formed by the compounds I and II mediated oxidation of tyrosine residues cannot oxidize it.

In summary, we have shown that etoposide can suppress cytochrome *c* catalyzed cardiolipin oxidation both in model systems and in cells only at rather high concentrations, exceeding those required for the induction of apoptosis. Thus etoposide-dependent inhibition of cardiolipin oxidation is not likely to interfere with the execution of apoptotic program and mitochondrial membrane permeabilization dependent on cardiolipin oxidation. Both cardiolipin peroxidation and etoposide oxidation by cytochrome *c*/cardiolipin complex predominantly involves protein derived radicals of cytochrome *c*. Because non-specific lipid antioxidants are not effective in inhibiting cardiolipin oxidation, other approaches based on the blockade of peroxidase reaction of cytochrome *c*/ cardiolipin complexes should be developed. In this regard, mitochondria-targeted nitroxide radicals capable of acting as selective acceptors of electrons from components of respiratory chain and preventing accumulation of superoxide and H₂O₂ may be promising (Wipf et al., 2005). Another interesting anti-apoptotic approach may be based on manipulations of cardiolipin fatty acid composition yielding its mono-unsaturated molecular species resistant to peroxidation (Kagan et al., 2005).

MOL (#22731)

References:

- Belikova NA, Vladimirov YA, Osipov AN, Kapralov AA, Tyurin VA, Potapovich MV, Basova LV, Peterson J, Kurnikov IV and Kagan VE (2006) Peroxidase Activity and Structural Transitions of Cytochrome c Bound to Cardiolipin-Containing membranes. *Biochemistry* **45**:4998 – 5009.
- Buettner GR (1993) The pecking order of free radicals and antioxidants: Lipid peroxidation, α -tocopherol and ascorbate. *Arch Biochem Biophys* **300**(2):535-543.
- Castner TGJ (1959) Saturation of the Paramagnetic Resonance of a V Center. *Phys Rev* **115**:1506–1515.
- Chen YR, Chen CL, Chen W, Zweier JL, Augusto O, Radi R and Mason RP (2004a) Formation of protein tyrosine ortho-semiquinone radical and nitrotyrosine from cytochrome c-derived tyrosyl radical. *J Biol Chem* **279**(17):18054-18062.
- Chen YR, Chen CL, Liu X, Li H, Zweier JL and Mason RP (2004b) Involvement of protein radical, protein aggregation, and effects on NO metabolism in the hypochlorite-mediated oxidation of mitochondrial cytochrome c. *Free Radic Biol Med* **37**(10):1591-1603.
- Egan RW, Paxton J and Kuehl FAJ (1976) Mechanism for irreversible self-deactivation of prostaglandin synthetase. *J Biol Chem* **251**(23):7329-7335.
- Garcia Fernandez M, Troiano L, Moretti L, Nasi M, Pinti M, Salvioli S, Dobrucki J and Cossarizza A (2002) Early changes in intramitochondrial cardiolipin distribution during apoptosis *Cell Growth Differ* **13**(9):449-455.
- Genova ML, Pich MM, Biondi A, Bernacchia A, Falasca A, Bovina C, Formiggini G, Parenti Castelli G and Lenaz G (2003) Mitochondrial production of oxygen radical species and the role of Coenzyme Q as an antioxidant *Exp Biol Med* **228**(5):506-513.
- Giulivi C, Traaseth N, J, and Davies KJA (2003) Tyrosine oxidation products: analysis and biological relevance. *Amino Acids* **25**(227–232).
- Gorman A, McGowan A and Cotter T (1997) Role of peroxide and superoxide anion during tumour cell apoptosis. *FEBS Lett* **404**(27-33).
- Griffiths SW and Cooney CL (2002) Relationship between protein structure and methionine oxidation in recombinant human alpha 1-antitrypsin. *Biochemistry* **41**(20):6245-6252.
- Jimenez CR, Huang L, Qiu Y and Burlingame AL (1998) In-gel digestion of proteins for MALDI-MS fingerprint mapping, in *Cur Prot Prot Sci* pp 16.14.11-16.14.15, John Wiley & Sons, Inc., New York.
- Kagan VE (1988) Lipid peroxidation in biomembranes, pp 1-181, CDC Press, Boca Raton, Florida.
- Kagan VE, Borisenko GG, Tyurina YY, Tyurin VA, Jiang J, Potapovich AI, Kini V, Amoscato AA and Fujii Y (2004) Oxidative lipidomics of apoptosis: redox catalytic interactions of cytochrome c with cardiolipin and phosphatidylserine. *Free Radic Biol Med* **37**(12):1963-1985.
- Kagan VE, Kuzmenko AI, Tyurina YY, Shvedova AA, Matura T and Yalowich JC (2001) Pro-oxidant and antioxidant mechanisms of etoposide in HL-60 cells: role of myeloperoxidase. *Cancer Res* **61**:7777-7784.
- Kagan VE, Tyurin VA, Jiang J, Tyurina YY, Ritov VB, Amoscato AA, Osipov AN, Belikova NA, Kapralov AA, Kini V, Vlasova II, Zhao Q, Zou M, Di P, Svistunenko DA, Kurnikov IV and Borisenko GG (2005) Cytochrome c acts as a cardiolipin oxygenase required for release of proapoptotic factors. *Nat Chem Biology* **1**(4):223-232.

MOL (#22731)

- Kagan VE, Yalowich JC, Borisenko GG, Tyurina YY, Tyurin VA, Thampatty P and Fabisiak JP (1999) Mechanism-based chemopreventive strategies against etoposide-induced acute myeloid leukemia: free radical/antioxidant approach. *Mol Pharmacol* **56**(3):494-506.
- Kagan VE, Yalowich JC, Day BW, Goldman R, Gantchev TG and Stoyanovsky DA (1994) Ascorbate is the primary reductant of the phenoxyl radical of etoposide in the presence of thiols both in cell homogenates and in model systems. *Biochemistry* **33**(32):9651-6096.
- Kalyanaraman B, Nemec J and Sinha BK (1989) Characterization of free radicals produced during oxidation of etoposide (VP-16) and its catechol and quinone derivatives. An ESR Study *Biochemistry* **28**(11):4839-4346.
- Kelso GF, Porteous CM, Coulter CV, Hughes G, Porteous WK, Ledgerwood EC, Smith RA and Murphy MP (2001) Selective targeting of a redox-active ubiquinone to mitochondria within cells: antioxidant and antiapoptotic properties. *J Biol Chem* **276**(7):4588-4596.
- Koppenol WH (1990) Oxyradical reactions: from bond-dissociation energies to reduction potentials. *FEBS Lett* **264**(2):165-167.
- Lassmann G, Odenwaller R, Curtis JF, DeGray JA, Mason RP, Marnett LJ and Eling TE (1991) Electron spin resonance investigation of tyrosyl radicals of prostaglandin H synthase. Relation to enzyme catalysis. *J Biol Chem* **266**(30):20045-20055.
- Malencik DA, Sprouse JF, Swanson CA and Anderson SR (1996) Dityrosine: Preparation, Isolation, and Analysis. *Anal Biochem* **242**:202-213.
- Niki E (1990) Free radical initiators as source of water- or lipid- soluble peroxy radicals. *Methods Enzymol* **186**:100-108.
- Nomura K, Imai H, Koumura T, Arai M and Nakagawa Y (1999) Mitochondrial phospholipid hydroperoxide glutathione peroxidase suppresses apoptosis mediated by a mitochondrial death pathway *J Biol Chem* **274**(41):29294-29302.
- Ott M, Robertson JD, Gogvadze V, Zhivotovsky B and Orrenius S (2002) Cytochrome c release from mitochondria proceeds by a two-step process. *Proc Natl Acad Sci U S A* **99**(3):1259-1263.
- Petrosillo G, Ruggiero FM and Paradies G (2003) Role of reactive oxygen species and cardiolipin in the release of cytochrome c from mitochondria. *FASEB J* **17**(15):2202-2208.
- Pham NA and Hedley DW (2001) Respiratory chain-generated oxidative stress following treatment of leukemic blasts with DNA-damaging agents. *Exp Cell Res* **264**:345-352.
- Raha S and Robinson BH (2001) Mitochondria, oxygen free radicals and apoptosis. *Am J Med Genet* **106**:62-70.
- Robinson NC, Zborowski J and Talbert LH (1990) Cardiolipin-depleted bovine heart cytochrome c oxidase: binding stoichiometry and affinity of cardiolipin derivatives. *Biochemistry* **29**:8962-8969.
- Scaffidi C, Fulda S, Srinivasan A, Friesen C, Li F, Tomaselli KJ, Debatin KM, Krammer PH and Peter ME (1998) Two CD95 (APO-1/Fas) signaling pathways. *EMBO J* **17**:1675-1687.
- Schlame M and Rustow B (1990) Lysocardiolipin formation and reacylation in isolated rat liver mitochondria *Biochem J* **272**:589-595.
- Svistunenko D, A. (2005) Reaction of haem containing proteins and enzymes with hydroperoxides: the radical view. *Biochim Biophys Acta* **1707**(1):127-155.
- Tsai AL, Wu G, Palmer G, Bambai B, Koehn JA, Marshall PJ and Kulmacz RJ (1999) Rapid kinetics of tyrosyl radical formation and heme redox state changes in prostaglandin H synthase-1 and -2. *J Biol Chem* **274**(31):21695-21700.

MOL (#22731)

- Tyurina YY, Serikan FB, Tyurin VA, Kini V, Yalowich JC, Schroit AJ, Fadeel B and Kagan VE (2004) Lipid antioxidant, etoposide, inhibits phosphatidylserine externalization and macrophage clearance of apoptotic cells by preventing phosphatidylserine oxidation. *J Biol Chem* **279**(7):6056-6064.
- Vlasova II, Tyurin VA, Kapralov AA, Kurnikov IV, Osipov AN, Potapovich MV, Stoyanovsky DA and Kagan VE (2006) Nitric oxide inhibits peroxidase activity of cytochrome c/cardiolipin complex and blocks cardiolipin oxidation. *J Biol Chem* [**Epub ahead of print**].
- Wardman P (1989) *J Phys Chem Ref Data* **18**:1637-1755.
- Wipf P, Xiao J, Jiang J, Belikova NA, Tyurin VA, Fink MP and Kagan VE (2005) Mitochondrial targeting of selective electron scavengers: synthesis and biological analysis of hemigramicidin-TEMPO conjugates. *J Am Chem Soc* **127**(36):12460-12461.
- Yalowich JC, Tyurina YY, Tyurin VA, Allan WP and Kagan VE (1996) Reduction of phenoxyl radicals of the antitumor agent etoposide (VP-16) by glutathione and protein sulfhydryls in human leukemia cells: implications for cytotoxicity. *Toxicol In Vitro* **10**:59-68.
- Zamzani N and Kroemer G (2003) Apoptosis: mitochondrial membrane permeabilization--the (w)hole story? *Curr Biol* **13**(2):R71-R73.

Footnotes: Supported by grants from NIH HL70755, NIH U19 AIO68021, CA90787, and GM64610.

MOL (#22731)

Legends for Figures

The reaction schema: Upon binding to an anionic phospholipid, cardiolipin, cytochrome *c*, is converted into a peroxidase, which in the presence of H₂O₂ catalyzes oxidation of cardiolipin, protein amino acids and other oxidizable compounds. As a result of the reaction of H₂O₂ with the heme of cytochrome *c*, highly reactive intermediates compound I and compound II are formed. The schema shows that in the etoposide can interact with protein-derived tyrosyl radical and/or lipid radicals to yield etoposide phenoxyl radicals. However, in the absence of etoposide, the reaction may proceed along one of the two pathways. Compounds I and II can oxidize protein amino acids, specifically tyrosine, (pathway 1), that can dimerize and form protein oligomers or abstract hydrogen from polyunsaturated cardiolipin (eg, TLCL) resulting in its peroxidation (pathway 2). The lipid alkyl radicals generated can form peroxy radicals under aerobic conditions and recombine with other lipid and protein radicals producing lipid and lipid/protein aggregates. Tyrosyl radicals are formed very effectively by compounds I and II and oligomerization proceeds mostly via pathway 1 in the absence of lipids or in the presence of non-oxidizable lipids (TOCL); when oxidizable polyunsaturated lipids (TLCL) are available, tyrosyl radicals effectively oxidize TLCL acyl chains.

Fig. 1. Effect of etoposide and AMVN on peroxidation of phospholipids in HL-60 cells and in liposomes. (A) A typical 2D-HPTLC of lipids extracted from HL-60 cells. 50 µg of phospholipids were used in the analysis. **NL**, neutral lipids; **CL**, cardiolipin; **PE**, phosphatidylethanolamine; **PC**, phosphatidylcholine; **SPH**, sphingomyelin; **PI**, phosphatidylinositol; **PS**, phosphatidylserine; **FFA**, free fatty acids. (B-C) Quantification of

MOL (#22731)

lipid peroxidation in HL-60 cells and liposomes. (B) HL-60 cells (2×10^6 /ml) or (C) liposomes composed of PAPC, PAPS and TLCL were incubated with either AMVN (500 μ M) or etoposide (25 μ M) or AMVN (500 μ M) plus etoposide (25 μ M) for 2h at 37°C. At the end of the incubation, lipids were extracted and separated by 2D-HPTLC. Phospholipid hydroperoxides were quantified by fluorescence HPLC using Amplex Red protocol. Data presented as Mean \pm S.E. (n=3); * $p < 0.001$ vs. control; # $p < 0.001$ vs. AMVN. (D) Etoposide induced caspase 3/7 activation and cytochrome *c* release (insert) in HL-60 cells. Cells were incubated in the presence of etoposide (25 μ M) for 2 h at 37 °C. At the end of the incubation, caspase 3/7 activity and cytochrome *c* release were measured by luminescence Caspase 3/7 kit and Western blotting, respectively. Data are presented as Mean \pm S.E. (n=3); *, $p < 0.01$ vs. control.

Fig. 2. Effect of etoposide on cardiolipin peroxidation induced by cytochrome *c*/cardiolipin complex in the presence of H₂O₂ or a lipid-soluble azo-initiator of peroxy radicals, AMVN. DOPC/TLCL (200 μ M, at a ratio of 1:1) liposomes were incubated in PBS at pH 7.4, containing 100 μ M DTPA with (A) AMVN (250 μ M) or in the presence of (B) cytochrome *c* (4 μ M) and H₂O₂ (100 μ M, 4 times every 15 mins) for 60 min at 37 °C. At the end of the incubation, lipids were extracted and hydroperoxides of cardiolipin were quantified by fluorescence HPLC using Amplex Red protocol. The degree of lipid peroxidation at different etoposide concentrations is presented as pmol CL-OOH/nmol cardiolipin. The control group represents liposomes without etoposide treatment. The data are presented as Mean \pm S.E. (n=3); *, $p < 0.001$ vs. control.

MOL (#22731)

Fig. 3. Etoposide-phenoxyl radicals production in presence of cytochrome *c*/TOCL and cytochrome *c*/ TLCL complexes. Liposomes (100 μ M DOPC and 100 μ M TOCL or TLCL) were incubated with etoposide for 15 min on ice. Then, cytochrome *c* (4 μ M) was incubated with liposomes for 1min at room temperature and the time course of EPR signal of etoposide radical was recorded for 4 min starting less than 1 min after addition of 100 μ M H₂O₂ (N₂ conditions). (A) EPR spectrum of etoposide phenoxyl radical (upper spectrum a), the underscored part of the spectrum was scanned repeatedly to measure the kinetics of etoposide radical formation (lower spectrum b) (B) Changes of the magnitude of etoposide radical EPR signal during 4 min measurements (see (A) lower spectrum) versus total etoposide concentration used in the experiment; DOPC/TOCL (\square) or DOPC/TLCL (\blacksquare) liposomes. Inset: Oxidation of TOCL and TLCL (hydroperoxide content) at (\square) 0min and (\blacksquare) 60 min after incubation with cytochrome *c* and H₂O₂. The data illustrated are from one representative experiment of a total of four experiments (with duplicate measurements for each etoposide concentration).

Fig. 4. Low temperature EPR measurements of phenoxyl radicals. (A) EPR-spectra of H₂O₂-induced phenoxyl radicals for cytochrome *c*/TOCL (a), cytochrome *c*/TLCL (b) or cytochrome *c*/TOCL in the presence of 500 μ M etoposide (c). Liposomes (5 mM, DOPC: 5 mM TOCL or TLCL) were incubated with cytochrome *c* (200 μ M) for 1 min at room temperature then H₂O₂ (1 mM) was added. Reaction was stopped after 20 s by freezing the samples in liquid nitrogen. (B) EPR spectra of nitrosylated cytochrome *c* in the presence of DOPC/TOCL (a) or DOPC/TLCL (b) liposomes. Ferro-cytochrome *c* (100 μ M) and DOPC/TLCL or DOPC/TOCL liposomes (2.5 mM at a ratio of 1:1) were incubated in 20 mM phosphate buffer (pH 7.4) containing DTPA

MOL (#22731)

(100 μ M) in the presence of PAPANONOate (500 μ M) under N₂ for 15 min at 37°C. The reaction was stopped by freezing the samples in liquid nitrogen and EPR spectra were recorded at 77K. (C) Power saturation curves of etoposide phenoxyl radical (○) and protein-derived tyrosyl radical (●) EPR signals. Saturation curves are the same for cytochrome *c*/TOCL and cytochrome *c*/TLCL complexes.

Fig. 5. Electrophoresis of cytochrome *c*/cardiolipin complexes. Liposomes (DOPC/TOCL or DOPC/TLCL) were incubated with cytochrome *c* (30 μ M and 4 μ M, for Coomassie blue and silver staining, respectively) (cardiolipin/cytochrome *c* at a ratio of 25:1) in PBS with 100 mM DTPA at 37°C for 1h and 100 mM H₂O₂ was added every 15 min. 15 μ l of the mixture were added to gel wells. Electrophoresis was performed using 12.5% SDS-PAGE with 5% stacking gel. A) Effect of etoposide on the formation of dityrosine cross-links in the incubation system TOCL/cytochrome *c* + H₂O₂ as compared to TLCL/cytochrome *c* + H₂O₂. Fluorescence at 420 nm (λ_{ex} 315 nm) was measured in the presence of varying concentrations of etoposide (0-250 μ M), TOCL (□) and TLCL (■). Data are Mean \pm S.E. (n=3); *, p< 0.005 vs. control (no etoposide). Inset: Dityrosine fluorescence of cytochrome *c* oligomeric cross-links formed in the presence of TOCL or TLCL after separation and elution from PAGE. Protein bands from Coomassie Blue stained gels were excised and cut into smaller pieces. Destaining, digestion with trypsin and extraction of peptides was performed. Dityrosines fluorescence of cytochrome *c*/TLCL in the presence of H₂O₂ and cytochrome *c*/TOCL in the presence of H₂O₂ was measured as described in Methods. Data are presented as dityrosine fluorescence intensity normalized to the content of protein in corresponding PAGE bands (as determined by densitometry of Coomassie Blue stained gels). Data are Mean \pm S.E. (n=3). (B) Typical SDS

MOL (#22731)

PAGE gels stained with Coomassie blue. (C) Integral density of monomeric cytochrome *c* bands of these samples (B). (D) Effect of etoposide of the formation of cytochrome *c* monomers (a) and aggregates (b) induced by H₂O₂ in the presence of TOCL or TLCL (Gels were stained with GelCode SilverSNAP Stain Kit II (Pierce)). Data are presented as % of control (pure cytochrome *c* sample), Mean \pm S.E. (n=3); *, p< 0.005 versus control.

Fig. 6. MS analysis of TLCL oxidation induced by cytochrome *c*/ H₂O₂ in liposomes.

TLCL/DOPC liposomes (1.5 mM at the ratio of 1:1) were treated with cytochrome *c* (30 μ M) and H₂O₂ (100 μ M was added four times every 30 min of incubation) in the absence and presence of etoposide (7.5-750 μ M). Lipids were extracted and accumulation of oxidized TLCL was quantified by fluorescence HPLC using Amplex Red protocol (A) and analyzed by mass spectrometry (B). The degree of cardiolipin peroxidation at different etoposide concentrations is presented as pmol CL-OOH/nmol cardiolipin. The control group represents liposomes without etoposide treatment. The data are presented as Mean \pm S.E. (n=3); *, *p* < 0.05 vs. control. Note: The significant accumulation of monohydroperoxy/monohydroxy derivatives of TLCL molecular species (B) as observed after incubation liposomes with cytochrome *c* and H₂O₂ (M/z 724.2 + 8 = 732.2; 724.2 + 16 = 739.7; 724.2 + 24 = 748.2; 724.2 + 32 = 755.9; 724.2 + 40 = 763.8; 724.2 + 48 = 771.8; 724.2 + 56 = 779.7; 724.2 + 64 = 787.9; and 724 + 72 = 795.7). This effect was markedly reduced by etoposide (750 μ M). Mass spectra prototypical of 3 independent experiments are presented.

Schema 1

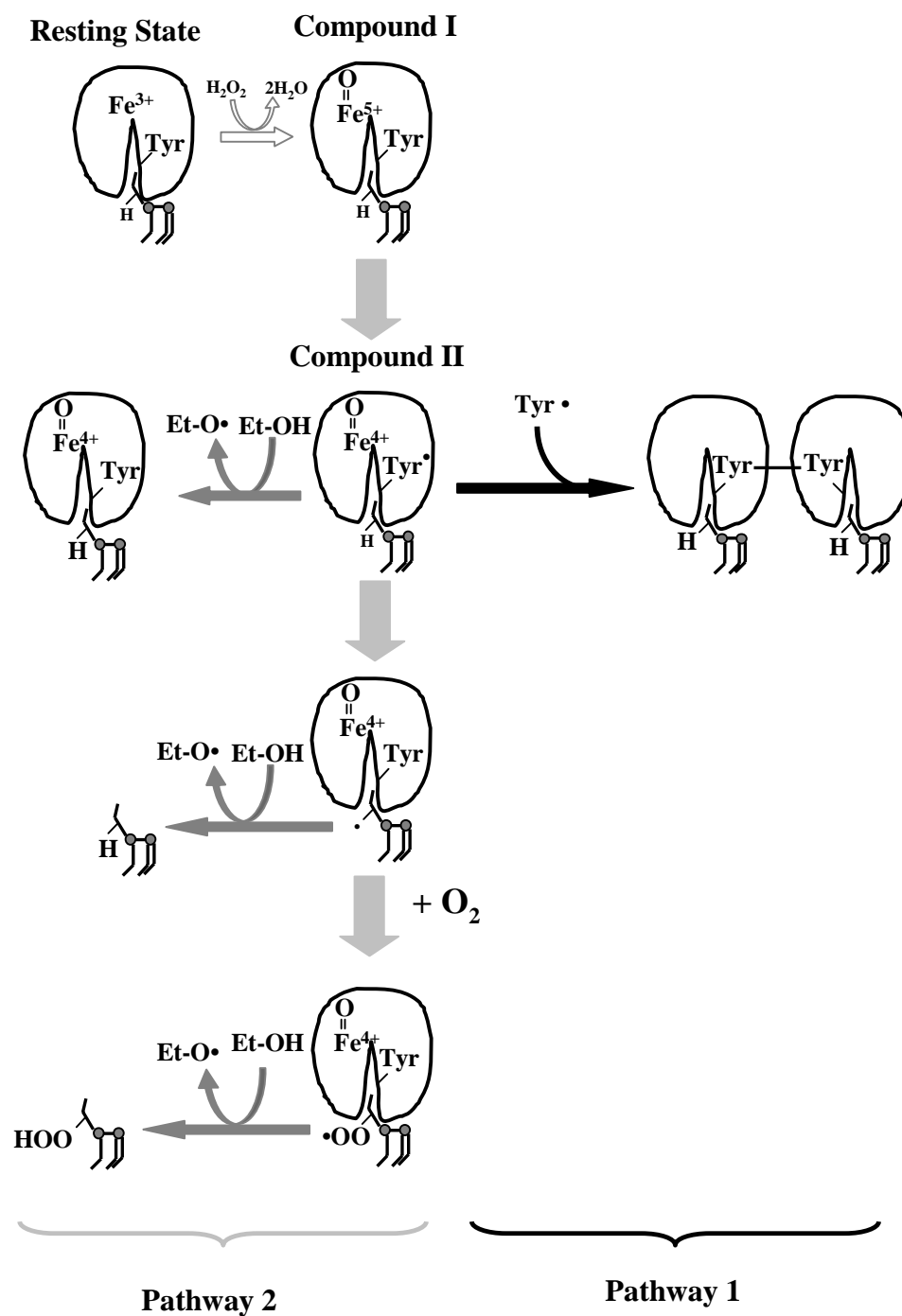


Figure 1

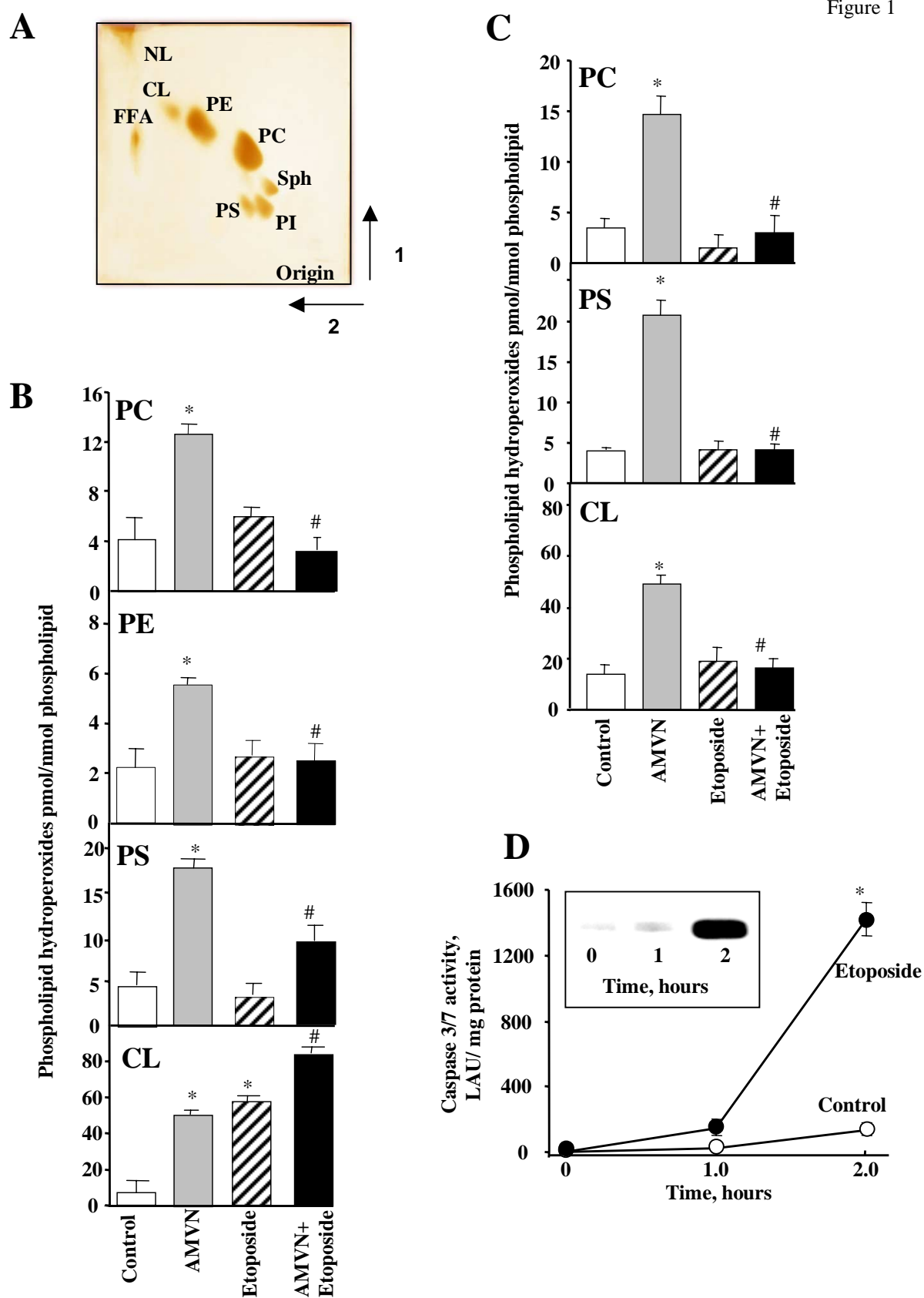
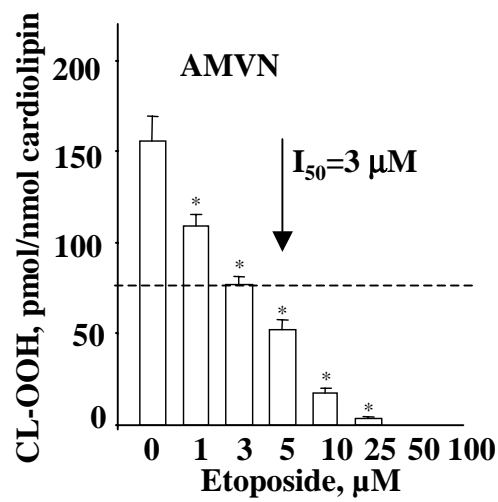


Figure 2

A



B

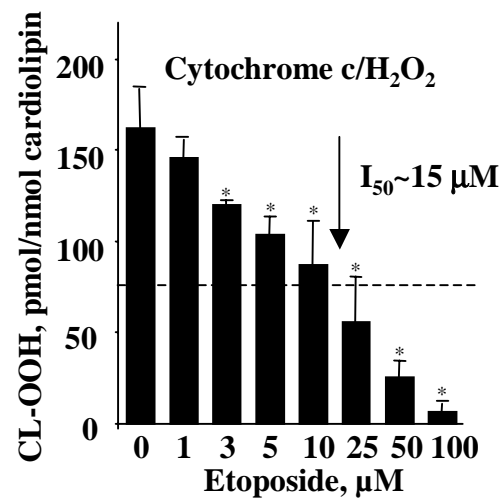


Figure 3

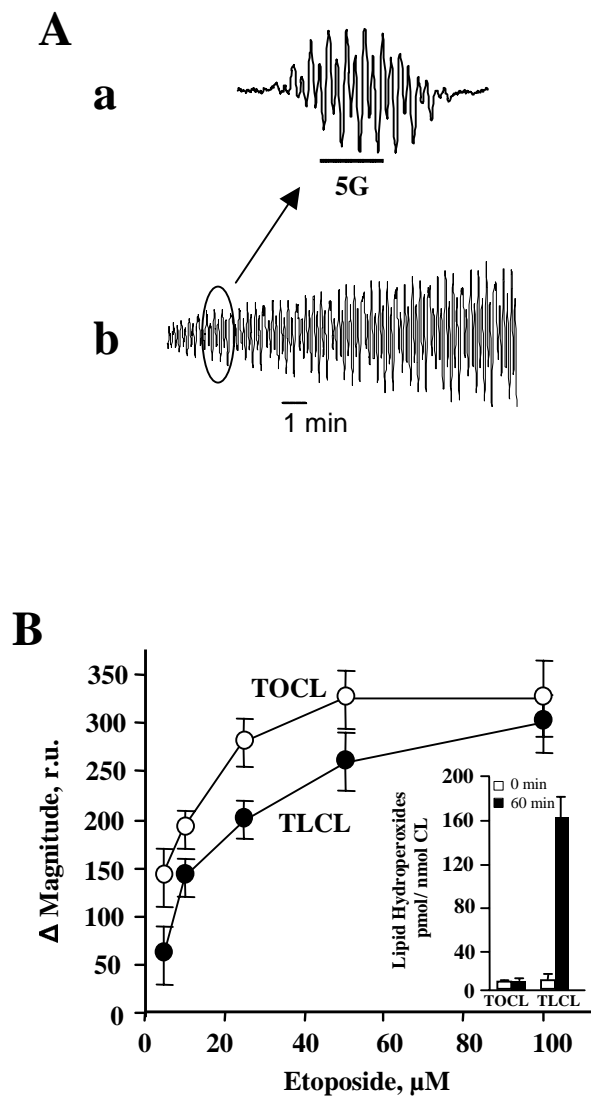


Figure 4

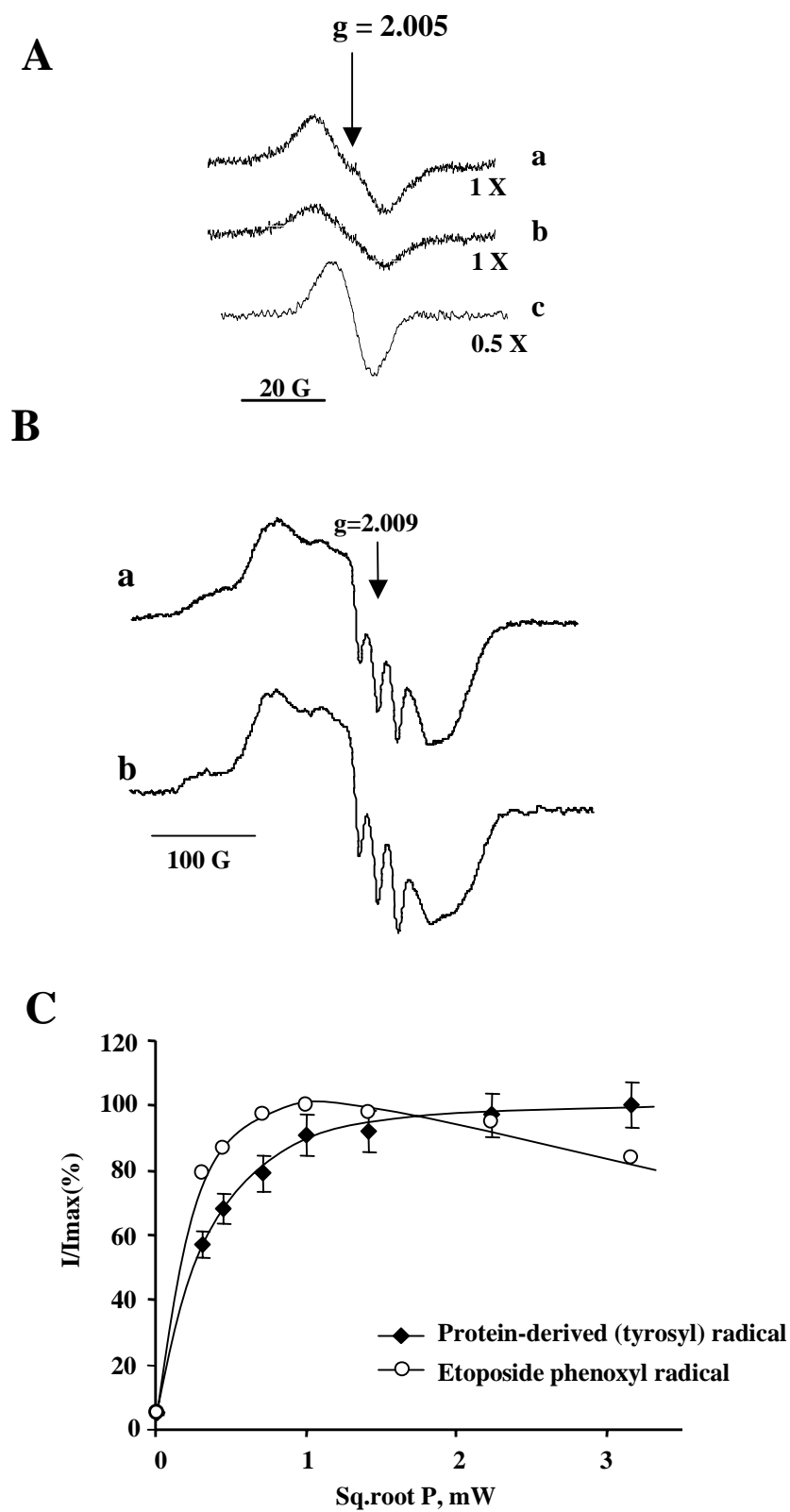


Figure 5

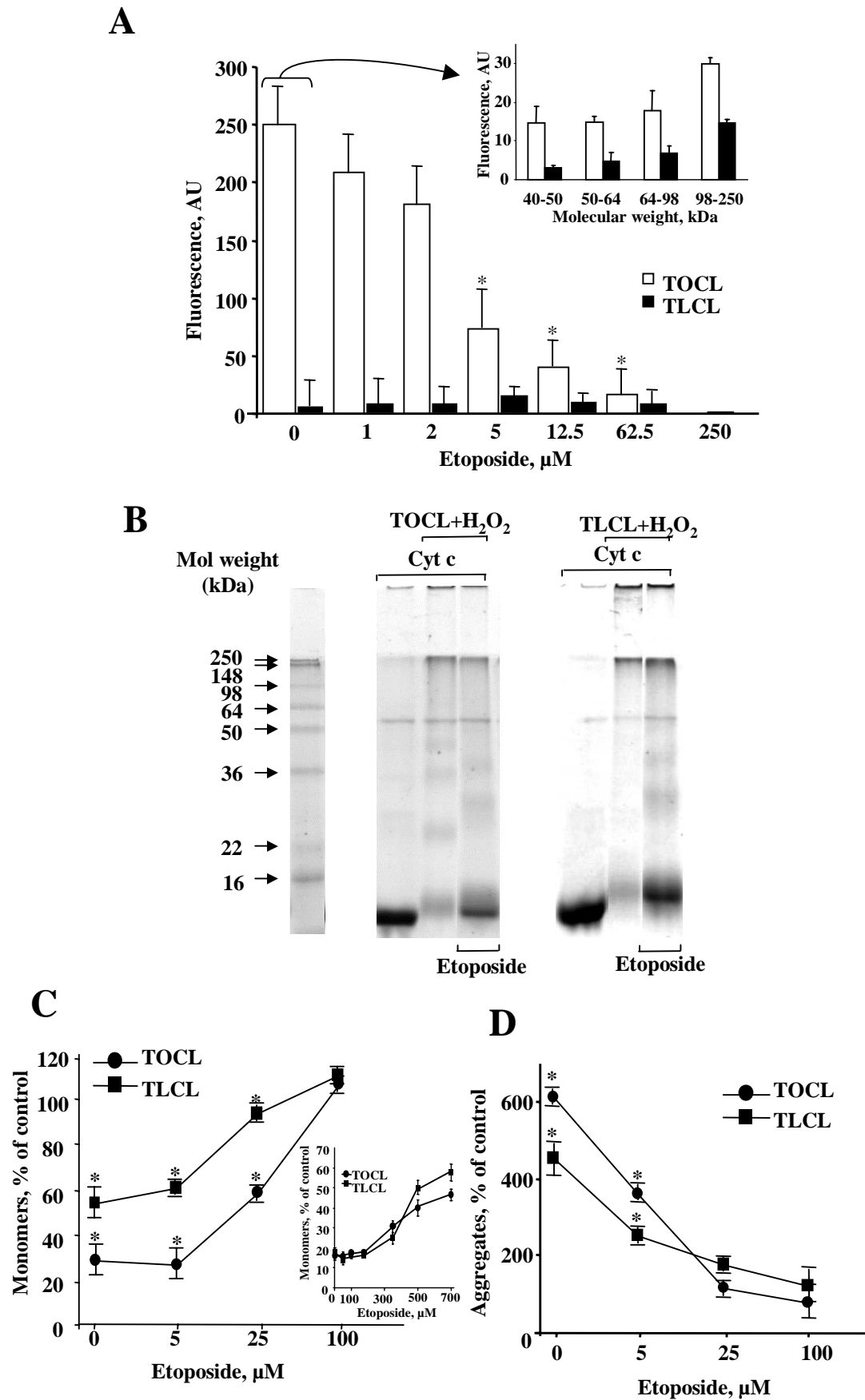


Figure 6

